frontiers | Frontiers in Earth Science

TYPE Original Research
PUBLISHED 07 November 2022
DOI 10.3389/feart.2022.1006930

Numerical assessment of riverbank filtration using gravel back filter to improve water quality in arid regions

Ismail Abd-Elaty[1], Osama K. Saleh[1], Hala M. Ghanayem[1], Martina Zeleňáková[2]* and Alban Kuriqi[3,4]

[1]Water and Water Structures Engineering Department, Faculty of Engineering, Zagazig University, Zagazig, Egypt, [2]Institute of Environmental Engineering, Faculty of Civil Engineering, Technical University of Košice, Košice, Slovakia, [3]CERIS, Instituto Superior Técnico, Universidade de Lisboa, Lisbon, Portugal, [4]Civil Engineering Department, University for Business and Technology, Pristina, Kosovo

Check for updates

OPEN ACCESS

EDITED BY
Ali Abedini,
Urmia University, Iran

REVIEWED BY
Mohamed Shamrukh Mahmoud,
Minia University, Egypt
Ahmet Sasmaz,
Firat University, Turkey

*CORRESPONDENCE
Martina Zeleňáková,
martina.zelenakova@tuke.sk

SPECIALTY SECTION
This article was submitted to Hydrosphere, a section of the journal Frontiers in Earth Science

RECEIVED 29 July 2022
ACCEPTED 20 September 2022
PUBLISHED 07 November 2022

CITATION
Abd-Elaty I, Saleh OK, Ghanayem HM, Zeleňáková M and Kuriqi A (2022), Numerical assessment of riverbank filtration using gravel back filter to improve water quality in arid regions. *Front. Earth Sci.* 10:1006930. doi: 10.3389/feart.2022.1006930

The main challenge of water resource management in high-stress regions, especially in developing countries, is in adopting non-traditional methods to obtain safe drinking water in desired quantities. In Egypt, the riverbank filtration (RBF) system is one of the most common solutions to solve rivers' water quality issues. Several sites have been investigated, and the system has demonstrated tremendous potential. The drinking water plant in Embaba, Giza, Egypt, is considered in this study to improve the quality of the abstracted water through the vertical well system. The numerical code of MODFLOW and MT3D is used to simulate the impact of using the emplacement of the gravel-pack filter (GPF). Three different scenarios were investigated: the first consists of vertical GPF; the second is horizontal GPF for different geometries, depths, widths or thicknesses, lengths, and permeability of the filter material; and, the third is drilling a pipe filter through the riverbed for different pipe numbers, depths, and the material's hydraulic conductivity. The results revealed that the riverbank filtration sharing (RBFS) rate was increased by increasing the filter width or thickness at the riverside, the filter pipe numbers, the length of the horizontal filter, and the permeability of filter material. At the same time, the thickness of the river bed decreased by increasing the filter width at the groundwater side. Also, the RBFS was increased by increasing the filter width or the thickness in the two directions and the pipe length. However, it returned to decrease again due to groundwater sharing. Thus, the RBF design should carefully consider the gravel-pack, pipe filter geometry, and permeability impact rate of RBFS.

KEYWORDS

riverbank filtration, groundwater, river sharing, MODFLOW, Embaba

1 Introduction

Water is an essential element that touches every aspect of our lives, from public health to safety and our economy's foundation. It is also the key component for human use, such as energy, industry, agriculture, and livestock (Hoff, 2009; Abd-Elaty et al., 2022a). Over three-quarters of Earth is water, but less than 3% is fresh water. In the last century, the population of the Earth has more than tripled, accompanied by a large increase in water demands, which has led to a large gap between the available and required quantities (Abd-Elaty et al., 2022b; Salehi, 2022). According to UNICEF, at least two and half billion people lack adequate sanitation, and more than a billion live without a potable water supply (Andrés et al., 2021).

The RBF technology has been utilized in Europe for decades, beginning in the 1870s in Germany to supply drinking water to cities along the Rhine, Elbe, Danube, and Seine rivers. In addition, the RBF remained one of the most efficient ways of providing high-quality drinking water following World War II, when rivers were extensively polluted (Ray et al., 2003; Ray, 2008; Abd-Elaty et al., 2021d; Poojitha et al., 2022). Many authorities worldwide have just begun assessing RBF's water treatment potential, especially in some developing countries like India, Jordan, and China (Abdalla and Shamrukh, 2010). It is a low-cost water treatment process that involves filtering the drinking water obtained from abstraction wells located near rivers, lakes, or ponds using existing geologic formations around rivers, lakes, or ponds. The bed and bank sediments filter the water bodies, eliminating pollutants. The procedure could produce potable water or serve as a reasonably basic pre-treatment for water to be further purified later. The obtained water is often of much higher quality than the raw surface water (Ray, 2011). The bank filtration is affected by geohydrologic conditions where the permeability of the sediment affects seepage velocity. Often, internal clogging is connected with sediments having low hydraulic conductivity and small vertical gradients. However, sediments with high conductivity will not be efficient in removing contaminants. There is an increasing interest in applying RBF because it can remove contaminants from surface water in low-cost processing technology as carried out in upper Egypt, particularly in Assiut Governorate since 2004, Sodfa city for 60 thousand inhabitants (Abdel-Lah and Shamrukh, 2006).

In that study and after 3 months of monitoring, RBF showed satisfactory chemical and microbial measurements. Turbidity, chemical species, alkalinity, hardness, and TDS readings were within allowed limits. For microorganisms, the efficiency of RBF in removing pathogens is noticeable. The capital and operational cost of this RBF compared to those of conventional water treatment plants are relatively low (Abd-Elaty et al., 2021d). These benefits from the RBF in the Nile Valley in Egypt make it a promising way to supply water without any prior treatment or treatment for high water quality. There are water quality issues in the Nile Valley with natural groundwater flow into the RBF wells. Therefore, the treatment and biochemical reactions occurring in this plant are unclear due to the interference of natural groundwater.

Further work is needed to identify guidelines for design considerations such as distance from Nile bank and pumping rate of wells. Traditional water purification plants failed to meet pressing environmental burdens despite the high cost. Initial processing is always insufficient (Mara et al., 1989). Water treatment plants face the following problems that greatly affect the quality of water produced, including the relatively high levels of alum dose and related problems concerning aluminum residues in water and the appropriately high costs of treated water. Moreover, relatively high levels of chlorine are added to raw water (i.e., pre-chlorination) to reduce the concentration of bacteria and fungi and similarly chlorine added to filtered water (i.e., post-chlorination). This increase in chlorine dose leads to an increased concentration of chlorinated organic compounds known as carcinogens (Sharma et al., 2021). The current water treatment processes are ineffective in removing pesticide residues and organic pollutants (Chaturvedi et al., 2021).

Moreover, they are insufficient to remove parasites, viruses, and other non-parasitic microorganisms. As a result, residual chemical and biological contaminants may remain in drinking water (Abdel-Shafy and Aly, 2002; Chaturvedi et al., 2021). Raw water with high levels of biological and chemical contaminants imposes a heavy burden on the efficiency of sand filters that block and develop microbial colonies, such as larvae of nematodes that may not be completely removed (Abdel-Shafy and Aly, 2002).

The filter pack surrounding the screen of pumping wells has an essential benefit, which is used to decrease the losses and increase the hydraulic efficiency of the well. For well construction, the filter zone is developed to remove fine particles, creating a turbulent flow zone and optimizing the efficiency, specific capacity, and safe yield of the pumping well. The gravel pack filter (GBF) surrounding the well screen may be provided in two ways:

The **first** is a naturally developed filter produced by removing the fine sand and silt from the aquifer material, bringing these fines through the well-screen openings by surging and bailing.

The **second** is the artificial pack type. An envelope of materials with a coarser uniform grain size than the aquifer is mechanically placed around the screen to filter the finer formation particles. Smith (1954) and Walton (1962) described the design criteria for either type based on the effective size, uniformity coefficient, and other grain-size distribution considerations determined from the mechanical analysis of the aquifer material.

Several methods have been suggested to determine the gravel pack grain sizes. All these are based initially on sieve analysis of the aquifer—the design filter based on (Terzaghi, 1943) following formula (ASTMD5447-17), Eq. 1.

$$\frac{D_{15\,\text{filter}}}{D_{85\,\text{aquifer}}} < 4 < \frac{D_{15\,\text{filter}}}{D_{15\,\text{aquifer}}}. \tag{1}$$

A common consensus is that a gravel pack will normally perform well if the uniformity coefficient based on the grain size distribution curves of the filter pack and the aquifer material is similar to that of the aquifer. The grain size of the aquifer material should be multiplied by a constant of approximately with an average value [4], Eq. 1, to create an envelope defining the filter grading.

Horizontal aggregation wells developed infiltration water supplies in the 1930s after oil engineer Liu Rani found that lower oil prices made the directly drilled horizontal wells less cost-effective (Tang et al., 2021). This method was modified from drilling horizontal wells in oil-bearing rock formations to hydraulic lifting. Perforated pipes are installed in underground water layer formations uncovered by sand and gravel. His theory, for both oil and water, was that if you could put the wells (i.e., open or sorting wells) in a horizontal configuration, you could expose the well to form the product, thereby developing higher returns for every single well as could be with one vertical well.

By 1953, an artificial gravel-pack filter was installed around the well screens of laterals in a horizontal collector well in Germany to accommodate fine-grained formations. A solid pipe is also projected full-length into the formation in this technique. The pipe is fitted with a particular well screen, and gravel materials are pumped into the annulus between the projection pipe and the screen, while the projection pipe is retracted. An artificial gravel-pack filter provides a transition between fine-grained formation deposits and more efficient screen openings.

This study presents a numerical assessment of RBF in the arid region of Cairo, Egypt, to improve drinking water quality and minimize treatment costs. The study was developed to simulate drinking water quality for RBF at the Embaba waterworks. Three potential scenarios to enhance the drinking water quality were simulated; the first is using a vertical gravel filter, the second is a horizontal gravel filter surrounding the RBF well, and the third is placing a pipe filter at the river's bed. In addition, the research provides simulation for a future RBF design to improve quality and reduce costs. The remainder of the study is structured as follows: Section 2 provides background information on the study case, including geological formation and water quality data, as well as a description of the methodology used; Section 3 presents the main findings and discusses their relevance and the effectiveness of the RBF technique. Finally, in Section 4, the main results from this study are presented.

2 Materials and methods

2.1 Study area

Nile Delta is about 2.8% of Egypt's area; the agricultural land presents about 67%, while the population is 63% of Egypt's population (Abd-Elaty et al., 2020). It is one of Egypt's significant oil- and gas-producing regions, also chemical industries, which is the main source of dangerous waste and water pollution in Nile branches and lakes due to agricultural pesticides, sewage, and effluents in urban and industrial areas (El-Sheekh, 2009; Abd-Elaty et al., 2022c). The case study lies in Giza Governorate, Egypt, between latitudes of 31° 4' to 31° 16' N and from 30° 4' to 30° 12' E. as shown in Figure 1.

Cairo has average temperatures in winter and summer between 12° and 31°C, respectively. So, the Nile Delta region is a warm zone and is generally dry, with an annual rainfall of less than 40 mm. The moisture ranges from 45 to 84%, while water evaporation rate is between 2.5 and 15 mm (El-Arabi et al., 2013; Alhejji et al., 2021).

2.1.1 Geological formation

The research area is in the southern section of the Nile Delta aquifer, which has been explored at various levels (RIGW, 1989, 1992; Said, 2012), and the Nile Delta area is covered with Quaternary deposits of Nile silt, clay, sandy clay, sands, and gravels. The Quaternary and Tertiary deposits, the top formation, are the two primary geological units in this region (Figure 2). The Holocene and Pleistocene sediments were found in the Quaternary deposits. Dunes, coastal deposits, sabkha deposits, and silty clay sediments cover the floodplain in the Holocene. At the same time, desert crusts, kurkar ridges, graded sand, and gravel surround the primary water-bearing structure in the Pleistocene. The Quaternary aquifer is around 100 m thick in Cairo and is 1,000 m thick along the shore. The Tertiary deposits, including Pliocene, Miocene, Oligocene, Eocene, and Paleocene sediments, make up the lower formation (Abd-Elaty et al., 2021f). The Pliocene is the major water-bearing formation's lower limit.

The Miocene deposits have a thickness of up to 2,000 m beneath the surface. However, the Oligocene and Eocene are not hydro-geologically significant since their groundwater contribution may be overlooked. However, it operates as a semi-constricting layer overlying the main aquifer. It is also quite productive, with an average thickness of 150 m and hydraulic conductivity ranging from 2.9104 to 1.1103 m/s (Kashef (1983).

2.1.2 Surface water quantity and quality

Surface water in Egypt is represented by the Nile, the main water supplier in Egypt. After the Nile Water Agreement in 1959 and the completion of the Aswan High Dam in the late 1960s, Egypt's share of the Nile's waters stabilized at 55.5 billion m^3 annually. While the actual discharge of the Aswan High Dam is roughly constant, irrigation needs are the main reason for the differing water discharge behind the dam, which fluctuates from 800 to 2,760 m^3/s during the winter and summer, respectively (El-Fadel et al., 2003). The fertilizers for irrigation water are major groundwater nutrients, providing about 8% of Egypt's revenue. On the other hand, precipitation is a limited water resource, except for the northern

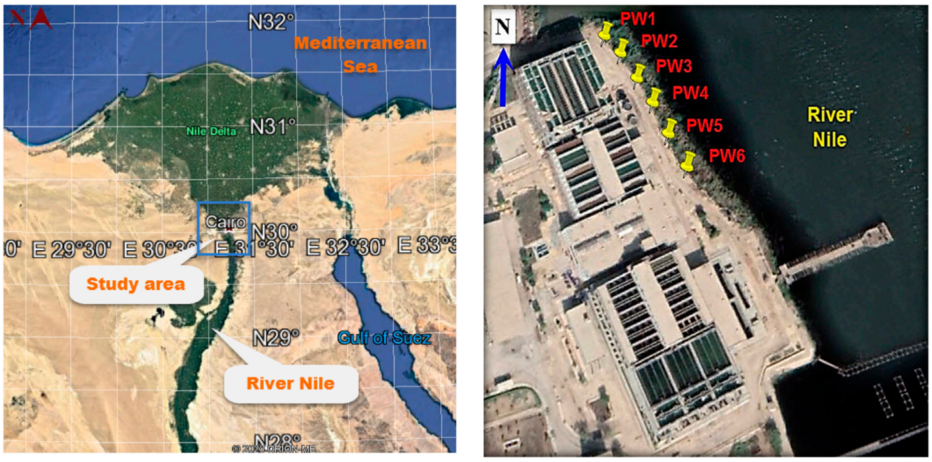

FIGURE 1
Location of the study case and the observation wells; PW1–PW6 represent the observation wells.

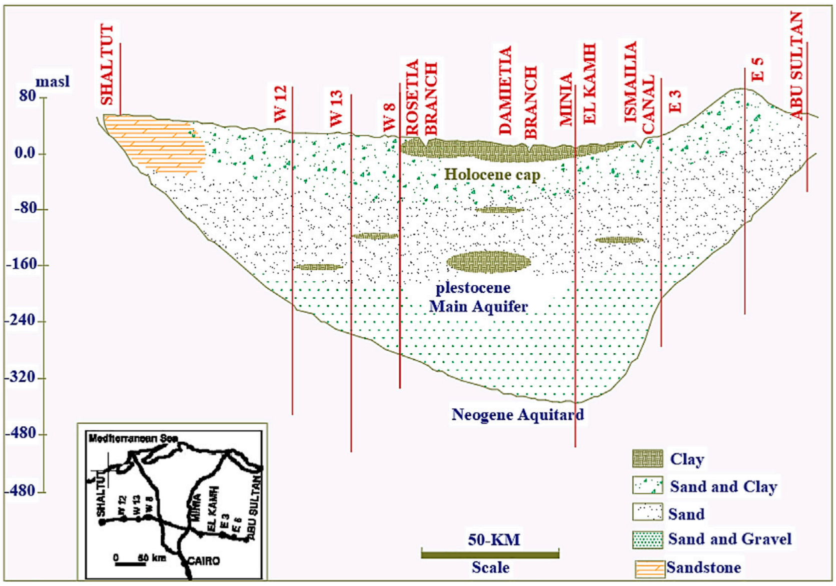

FIGURE 2
Regional hydrogeologic cross-section illustrating the main aquifer of the Nile Delta after Ghodeif et al. (2018).

parts of Egypt, which are subjected to winter rains (Wahaab and Badawy, 2004; Abd-Elaty et al., 2021b). Pollution from various sources, including industrial wastewater, oil pollution, native water pollution (Abd-Elaty et al., 2019), and agrarian pollution, contributes heavy metals, pesticides, herbicides, and bacteria to the river Nile. Excess nutrients trigger the blooming of blue-green algae, resulting in the formation of cyanotoxins, which harm aquatic creatures and may poison humans (El-Sheekh, 2009). The Nile's surface and groundwater has rapidly deteriorated due to the growing discharge of filthy home and industrial wastes. Egypt is the Nile's most industrial country. The industrial sector's water requirements were projected by the Ministry of Water Resources and Irrigation to be 5.4 BCM of water used by Egypt's industrial sector each year (MWRI, 2017), with 85% of the water being released into drainage systems that flow into the rivers again (Wahaab and Badawy, 2004).

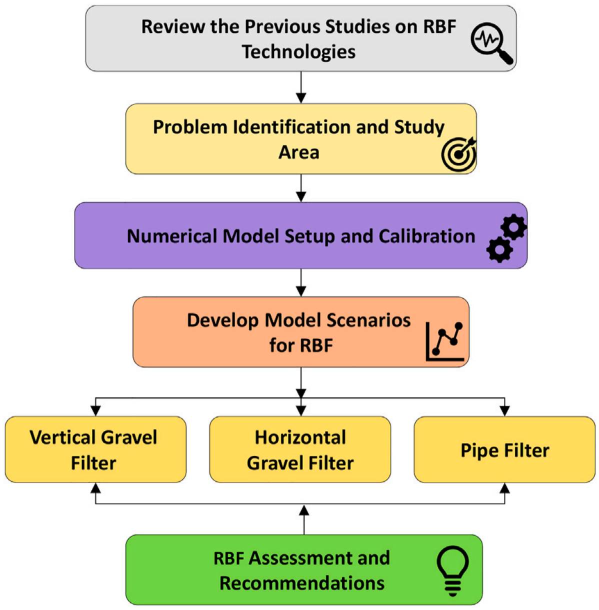

FIGURE 3
Flow chart shows the methodological approach applied in this study.

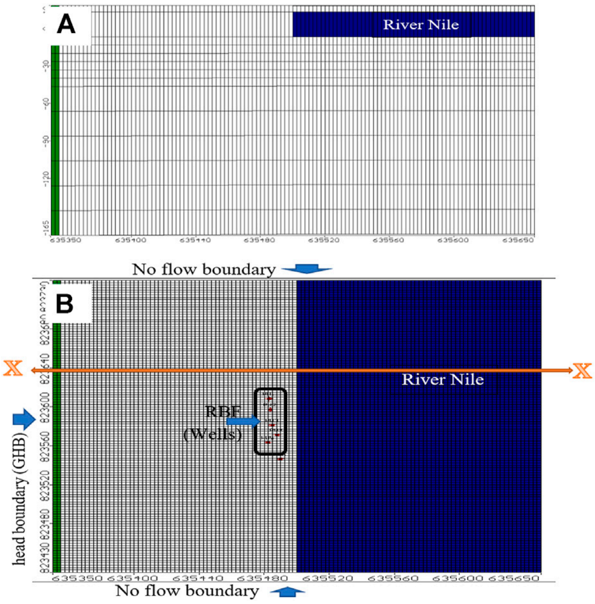

FIGURE 4
Study area digitizing and boundary condition: **(A)** aerial view and **(B)** section in X-X direction.

2.1.3 Installation of an RBF scheme at Embaba, Giza

In order to test the viability of using RBF at the Embaba waterworks to fulfill Cairo's rising water demand, the Holding Company for Water and Wastewater drilled a total of six pumping wells (Figure 2B) parallel to the Nile riverbank. Wells were drilled [10–15 m] away from the riverside; they have submersible pumps with a planned average discharge of 150 m^3/h, a 400-mm casing diameter, a 450-mm drilling diameter, and an average depth of 54 m (i.e., 24 m casing, 24 m screen, and 6 m sand trap).

Over 1.5 years, water samples were only frequently taken because they had to be taken at least once every quarter to meet specific criteria. Many of the data could not be systematically analyzed because the RBF wells could not be run continuously or regularly. Analyses of water quality standards were carried out by the central laboratory of the Giza Water and Wastewater Company and the main reference laboratory of the Holding Company for Drinking Water and Wastewater (Paufler et al., 2018; Abd-Elaty et al., 2021a).

2.2 Methodology

Figure 3 presents the methodological approach that begins with assessing previous studies related to RBF technologies and identifying recommendations that could be potentially tested in our study case.

Then, we identified a study where the different recommendations and RBF technologies could be tested. Afterward, model setup and calibration were carried out, where several simulations were conducted for three different filter scenarios. Finally, recommendations were provided regarding the design and implementation of RBF in arid regions.

2.2.1 Model for simulating groundwater flow and transport

Numerical modeling is used to simulate the groundwater flow and solute transport problems (Abd-Elaty and Straface, 2022). The RBF water quality was simulated for the current situation and three scenarios using a numerical model to examine the viability of this system. It was simulated first by MODFLOW for hydraulic and flow simulation. The solute transport model and the partial differential equation were simulated using the MT3D code (Javandel et al., 1984), Eq. 2.

$$\frac{\partial[\theta C^k]}{\partial t} = \frac{\partial}{\partial x_i}\left[\theta D_u \frac{\partial C^k}{\partial x_j}\right] - \frac{\partial}{\partial x_i}\left[\theta V_i C^k\right] + q_s C_s^k + \sum R_n, \quad (2)$$

where C^k is the dissolved concentration of species k, ML^{-3}; Ɵ is the porosity of the porous medium, dimensionless; t is time, T; D_u is the hydrodynamic dispersion coefficient, $L^2 T^{-1}$; V_i is the seepage or linear water velocity, LT^{-1}; it is related to the specific discharge or Darcy flux through the relationship. q_s is the volumetric flux of water per unit volume of aquifer representing sources (positive) and sinks (negative); $[T^{-1}]$ is

TABLE 1 Hydraulic parameters of the study area (El-Atfy, 2007; Mabrouk et al., 2018).

Main hydraulic units	Layer #	Hydraulic conductivity		Storage coefficient	Specific yield	Effective porosity
		K_h(m^2 day^{-1})	K_v (m^2 day^{-1})	S (--)	Sy (m^{-1})	n (%)
Clay	1	0.25	0.025	3–10	0.1	40
Fine sand with a lens of clay	2,3	5–25	0.5–2.5	5×10^{-3}	0.15	35
Coarse sand Quaternary	4,5,6	40–60	4–6	2.5×10^{-3}	0.2	25

the concentration of the sources or sinks of species k, ML^{-3} and R_n is chemical reaction term, $ML^{-3}T.^{-1}$

2.2.2 Configuration

The groundwater flow model domain was 300 m^2 in size or 300 m in length by 300 m in width. The square mesh size ranges from 5 m to 25 m^2, divided into 60 columns and 60 rows, each displayed in (Figure 4). Six layers make up the aquifer depth. While the subsequent layers of the Quaternary aquifer have a thickness of roughly 42 m, the initial layer represents the clay cap and is 5 m thick.

2.2.3 Boundary conditions and hydraulic parameters

The present model's boundary conditions were established using a river package, with the Nile River assigned at the east side and stage starting by [16.17 m] above mean sea level (a.m.s. l) at the south to (16.15 m), slopes of the Nile River was set to 0‰. The real slope is estimated to be 0.02‰ (Ghodeif et al., 2018); it is too small and, as a result, is ignored for modeling at the northern and southern edges has no-flow bounds. However, a general head boundary is present along the western model boundary, i.e., GHB, Cauchy BC represented the affected groundwater headset 16.18 m (a.m.s.l) at 150 m from the Nile. Figure 4 shows the study area boundary conditions, while the two sections in the *X* and *Y* direction were presented.

Table 1 shows the hydraulic characteristics of the aquifer, including hydraulic conductivity. [K], storage coefficient [S], specific storage [Ss], and effective porosity; these parameters are reported by El-Atfy, (2007); Morsy, (2009); Abd-Elaty et al., (2021e).

In contrast to the normal recharge rate of 0.30 mm/day into the aquifer's water table, the total abstraction from the current area reached 50,000 m^3/day. A constant concentration of TDS with a value of 260 ppm was assigned along the river boundary (Ghodeif et al., 2018), which presents the value of TDS contamination in the Nile River. The contaminant recharge and initial concentration were set at 1000 ppm as an initial value for the TDS concentration in the groundwater.

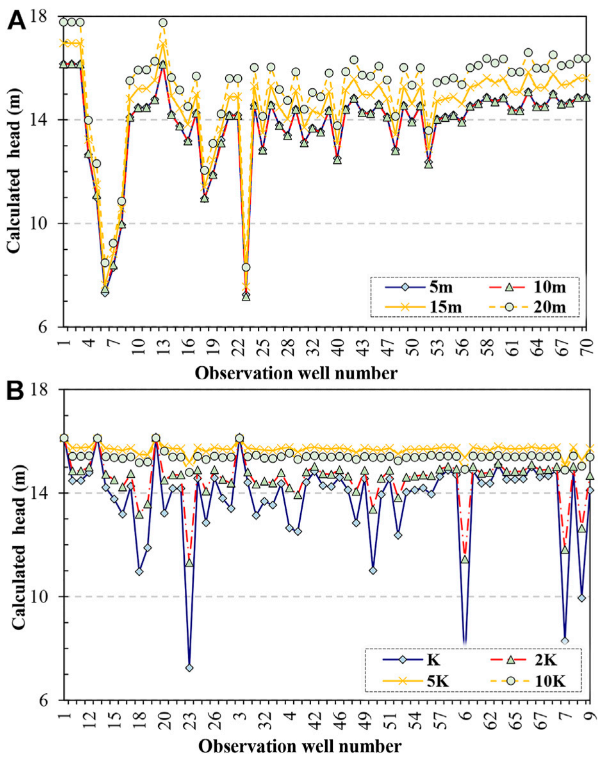

FIGURE 5
Model sensitivity for **(A)** grid size and **(B)** hydraulic conductivity.

2.2.4 Model sensitivity

This step involves a perturbation of model parameters to see how much the model results change. The groundwater flow model was examined by checking the effect of grid size on the stability of the model results; also, the uncertainty of parameters for hydraulic conductivity and porosity was checked.

The current model was digitized by changing the grid size by 20, 15, 10, and 5 cm to examine the stability of the model; the model results showed that decreasing the model grid size

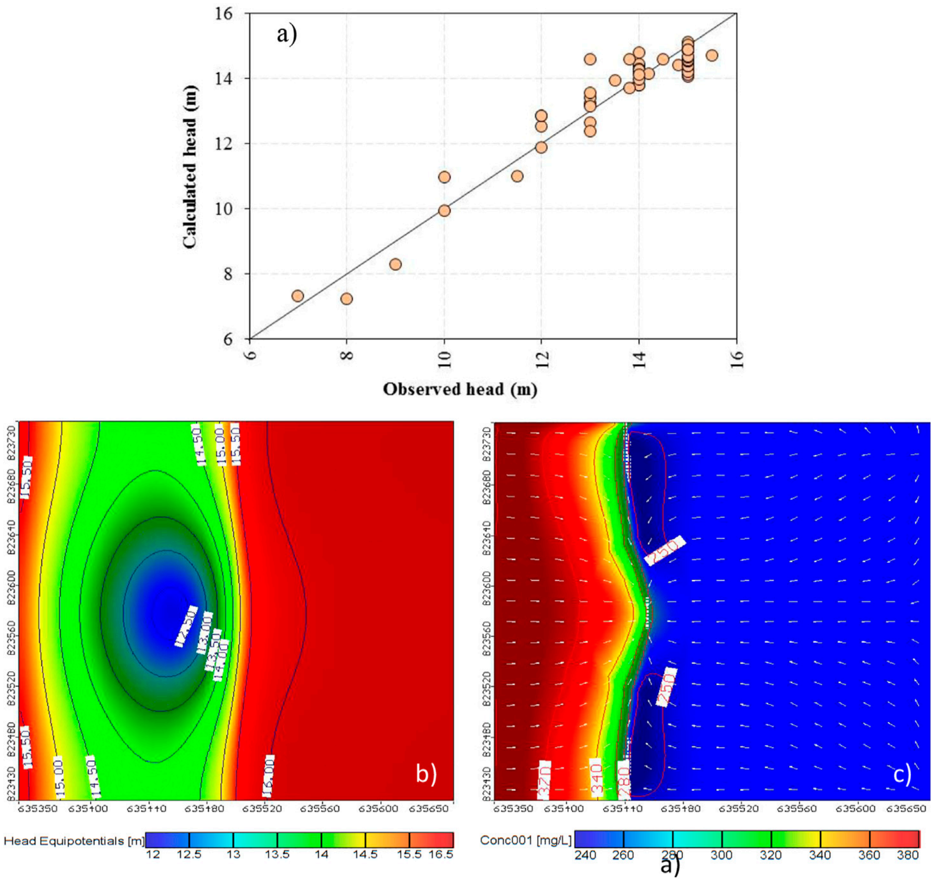

FIGURE 6
Model results for RBF at the Embaba site: **(A)** calculated vs. observed head, **(B)** groundwater head, and **(C)** TDS distribution.

increased the accuracy of model calibration, as presented in Figure 5A.

Moreover, the model hydraulic conductivity (Figure 5B) was checked by changing the values by 0.10 k and 10 K from the basic values presented in Table 1. The results showed that increasing the hydraulic conductivity is a more effective parameter in the calibration process. At the same time, the effect of porosity is very low and has little effect on model calibration.

2.2.5 Model calibration

The model calibration was started by comparing the simulated head with the measured data from the observation wells (Abd-Elaty et al., 2021g). These recorded data were developed using the Piezometric Contour Map in Greater Cairo (El-Arabi et al., 2013). Figure 6A shows the difference between the calculated and observed heads. The root mean square [RMS] and normalization root mean square reached 0.504 m and 5.54%, respectively.

The correlation coefficient reached 0.962. The flow model was calibrated using MUDFLOW for steady-state by changing the aquifer hydraulic conductivity by trial and error to match the model results and piezometric head, as shown in Figure 6B; the reason for selecting the hydraulic conductivity is based on the sensitivity analysis which is a critical parameter effect on the model calibration. The results demonstrate that the river zone experiences high water levels. At the same time, the westside neighborhoods of Nadi El Remaya and El Golf Club have low water levels. The field data from the RBF results were used to calibrate the solute transport model. In the current simulation, the total dissolved solid [TDS] as the quality and contamination parameter was chosen and reported by (Ghodeif et al., 2018; Paufler et al., 2018; Abd-Elaty et al., 2021c). The results of MT3D showed satisfactory agreement with the field data (Figure 6C).

2.2.6 Estimation of the hydraulic conductivity of the filter

To simulate the model's emplacement of the gravel river pipe, we changed the hydraulic conductivity value of the model's cells. We studied the effect of changing the numbers, the depth, and the hydraulic conductivity values in the range of filter values.

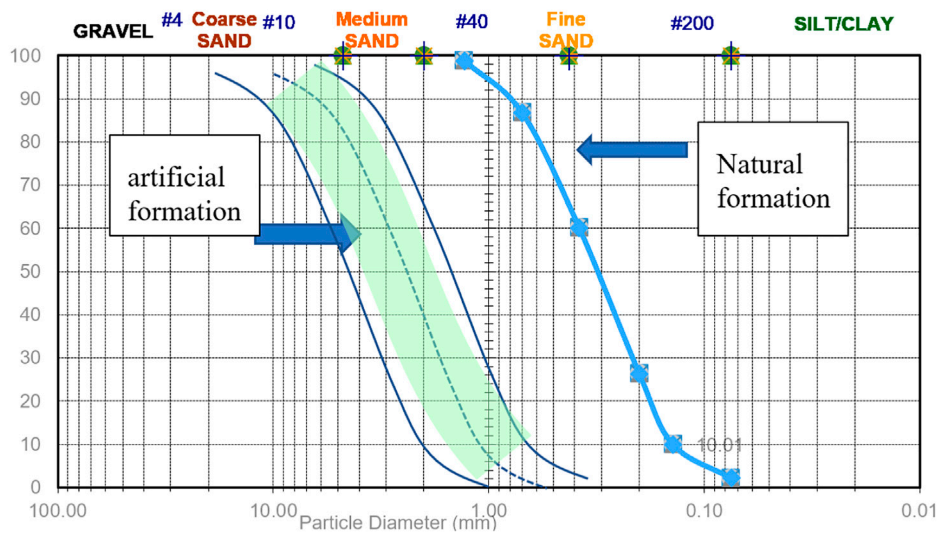

FIGURE 7
Grain size distribution curve at the Embaba site.

Ghodeif et al. (2018) illustrated the results of the grain size analysis and an assessment of the aquifer's hydraulic conductivity in the area of the pumping wells, concluding that an artificial gravel pack is necessary due to

- first—Uniformity Coefficient Cu= D_{60}/D_{10} = 0.52/0.22= 2.36 < 3.

- Second—D_{10} =0.22 < 0.25 mm.

Using the grain size distribution curve (Figure 7), we could calculate the hydraulic conductivity of the filter from the Hazen formula, Eq. 3.

$$K_H = C_H * D_{10}^2. \tag{3}$$

Where K_H is hydraulic conductivity [cm/s], C_H is an empirical coefficient equal to 100 [$cm^{-1}s^{-1}$], and D_{10} is the particle diameter of the filter at 10% passing measured in centimeter. As reported by Carrier III, (2003), C_H is commonly given as 100. However, published values range over two orders of magnitude from 1 to 1000 $cm^{-1}s^{-1}$. The Hazen formula is assumed valid for 0.1 mm ≤ D_{10} ≤ 3 mm and C_U ≤ 5.

The filter was simulated by changing the cells' hydraulic conductivity [Kf] around the RBF wells.

2.2.7 Definition of model scenarios

To simulate the emplacement of a gravel pack filter in the study area of the Embaba drink water plant, the hydraulic conductivity value was changed for the model's cells to study the effect of changing the hydraulic conductivity's width, depth, and the range of filter values.

A total of five scenarios were carried out to assign a gravel filter with RBF technology. The main parameters are filter width and depth dimensions, hydraulic conductivity with the repetition of these scenarios on the horizontal filter, and the drilled pipe's depth, numbers, and hydraulic conductivity. Table 2 presents the scenarios applicable to vertical and horizontal gravel filters and drilled pipes based on the main parameters affecting filter efficiency.

As shown in Figure 8A, the first is to change the filter width [W] in the riverside, and the groundwater side increases to 2.5 m [cell size] from the base case of 10 m.

The second is to change the width of the filter on both sides by increasing it to 5 m for each side while changing the horizontal filter depth [D] by 24, 32, 34, 39, and 42 m from the base case, which is 30 m. Also, the length of the horizontal filter was changed to 80, 90, 100, 110, and 120 m compared with 70 m at the base case. The third parameter is the hydraulic conductivity of the gravel filter [K], which is changed by 10, 30, 50, 100, and 120 m/day from the base pack (74 m/day) (Figure 8B). Figure 8C shows the main parameters to assess the drilled pipe efficiency: pipe numbers, depth, and hydraulic conductivity of the pipe material. Table 2 summarizes these scenarios; the numbers of the river pipe [N] changed with 1, 3, 5, 7, 9, and 11 while increasing the pipe depth [D] 51, 61, 71, 81, and 91 m, respectively, from the base case of 41 m. The third parameter is the hydraulic conductivity of the gravel filter [K], changing the hydraulic conductivity values by 10, 30, 50, 100, and 120 m/day from the base pack [74 m/day].

The efficiency of using a gravel filter or river pipe on pumped water quality was calculated using the mean value of TDS (ASTMD5447-17, 2017) and as shown in Eq. 4:

TABLE 2 Different proposed scenarios for filter emplacement.

Case	Filter type	Description	Base case	Scenarios #				
				1	2	3	4	5
Width [m]	Vertical	River or GW side [W]	10	12.5	15	17.5	20	22.5
		Both sides [W]		15	20	25	30	35
Depth [m]		D	30	24	32	34	38	42
Permeability [m/day]		K	74	10	20	30	50	100
Thickness [m]	Horizontal	Upward or downward [T]	10	12.5	15	17.5	20	22.5
		Both sides [T]		15	20	25	30	35
Length [m]		L	70	80	90	100	110	120
Permeability [m/day]		K	74	10	20	30	50	100
Number	Pipe	N	7	1	3	5	9	11
Depth [m]		D	41	51	61	71	81	91
Permeability [m/day]		K	74	10	30	50	100	120

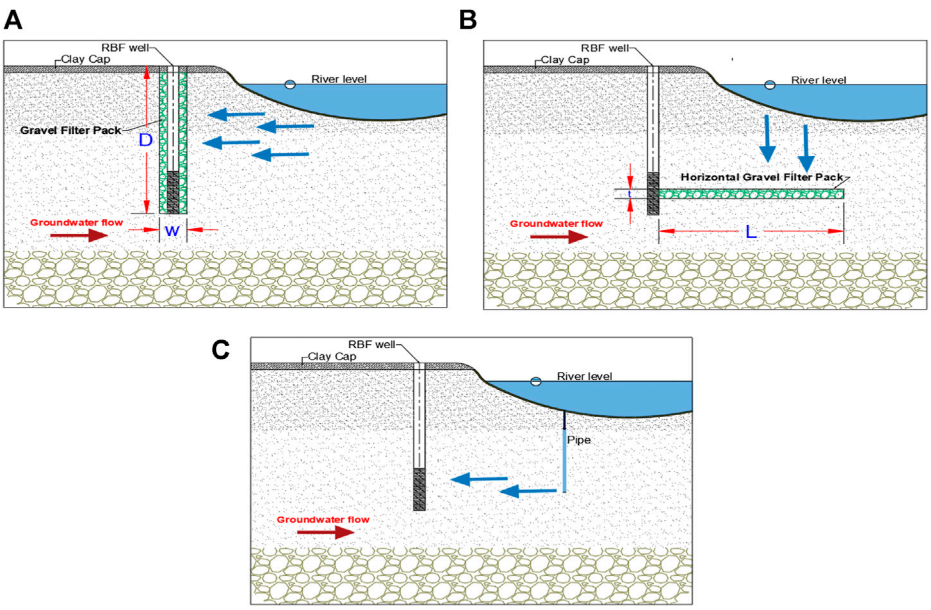

FIGURE 8
Proposed scenarios for the RBF gravel pack and pipe filter at the Embaba site are **(A)** vertical gravel filter, **(B)** horizontal gravel filter, and **(C)** pipe filter.

$$FE\% - RPE\% = \frac{(TDS)_{\text{aquifer}} - (TDS)_{\text{filter-pipe}}}{(TDS)_{\text{aquifer}} - (TDS)_{\text{River}}}, \quad (4)$$

where FE% is the filter efficiency, RPE% is the river pipe efficiency, $[TDS]_{\text{aquifer}}$ is the concentration of Total Dissolved Solid in the aquifer around the pumping well, $[TDS]_{\text{filter-pipe}}$ is the concentration of TDS in pumped water due to using a filter or pipe, and $[TDS]_{\text{River}}$ is the concentration of TDS in surface water or river.

3 Results and discussion

3.1 Effect of filter width/thickness on filter efficiency

The results of changing the vertical filter width and the thickness of the horizontal packing filter are shown in Figures 9A,B, where the filter width [W] and thickness [T] in riverside were increased by 12.5, 15, 17.5, 20, and 22.50 m. The RBFS %

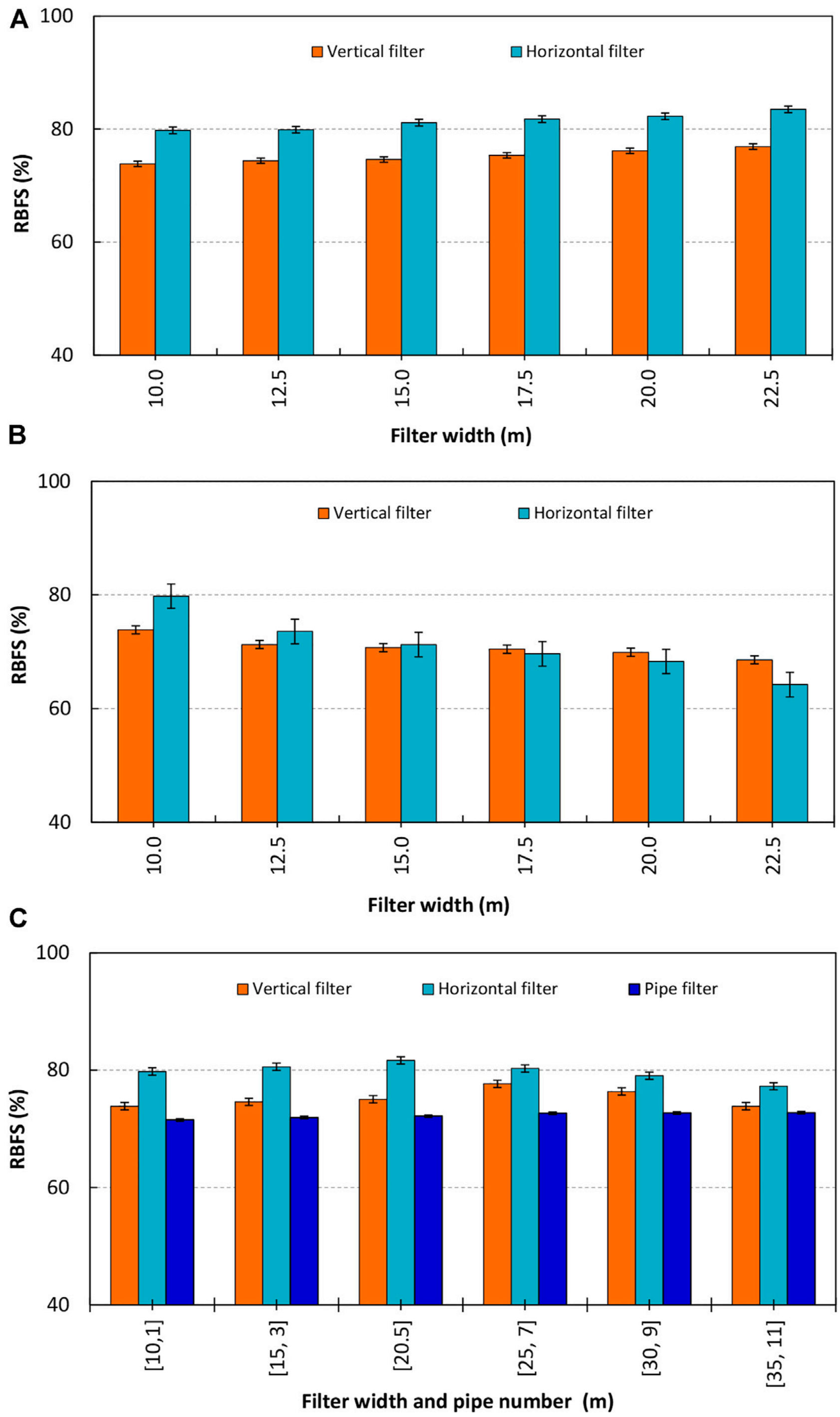

FIGURE 9
Riverbank filtration efficiency for **(A)** filter width riverside, **(B)** filter width groundwater side, and **(C)** filter width both sides and river pipe numbers.

increased to 74.40, 74.70, 75.40, 76.20, and 77% compared with 73.90% (≈10 m) for the vertical filter at the base case. In contrast, in the horizontal case, the RBFS % reached 80, 81.20, 81.80, 82.30, and 83.50% compared with 79.80% at the base case of the horizontal filter [10 m], which indicates that increasing the filter width or thickness at the riverside increases the possibility for high-quality drinking water by the sharing of the river compared with the groundwater (Figure 9A).

Increasing the filter width or thickness in the groundwater side by 12.5, 15, 17.5, 20, and 22.50 m has decreased RBFS to 71.30, 70.80, 70.50, 70, and 68.60%. For the vertical filter, the RBFS % reached 73.60, 71.50, 69.60, 68.30, and 64.20%, compared with 73.90% (≈10 m) and 79.80% (≈10 m) for the vertical and horizontal filter at the base case (Figure 9B), respectively, which indicated that increase the filter width at the aquifer side has decreased the RBFS due to the increase in the groundwater sharing compared with the river water.

Moreover, increasing the filter widths or thickness in both directions for river and groundwater sides by 15, 20, 25, 30, and 35 m caused the RBFS% to be 74.60, 75.10, 77.70, 76.30, and 73.80% in the vertical filter and 80.60, 81.70, 80.20, 79, and 77.20 for the horizontal filter, respectively. The RBFS at the base case reached 73.90% (≈10 m) and 79.80% (≈10 m) for the vertical and horizontal filters, respectively. This indicates that the RBFS was increased due to the effect of the filter width for increasing the water quality and increasing the effect of river sharing but increasing the width or thickness then it was followed by decreasing the RBFS due to the effect of groundwater sharing in the aquifer side and subterranean bottom layers (Figure 9C).

On the other hand, changing the numbers of the river pipe filter by 1, 3, 5, 7, 9, and 11 shows the effect of using the river pipe on the efficiency of the RBF system, whereby increasing the river pipe number effect on the RBFS% recorded 71.53,7 1.92, 72.18, 72.66, 72.71, and 72.76% at 1, 3, 5, 7, 9, and 11, respectively, compared with 71.47% without using river pipe, indicating a possibility of obtaining water with high quality by using this technique (Figure 9C).

3.2 Effect of filter depth and length on RBF water quality

The scenario was simulated using MDFLOW/MT3D models by changing the vertical filter depth by 24, 32, 34, 38, and 42 m. The results show that increasing the filter depth increased the efficiency of RBFS by 71.30, 75.20, 77.70, 80.30, 75.10, and 73.80%, compared with 71.50% at the base case (≈30 m). This can be interpreted due to the effect of the clay layer at the top and the groundwater at the bottom. For increasing the length of the horizontal filter in river direction by 80, 90, 100, 110, and 120 m, it recorded an increase in RBFS to reach 79.80, 81, 82.40, 84.50, and 87.70%, respectively, compared with 79.80% at the base case (≈70 m). The effect of river seepage can explain this by increasing the infiltration length, enabling river water to enter directly to the wells and increasing the sharing of RBF from the river (Figure 10).

Furthermore, changing the pipe depth from 41 to 91 m by increasing the depth to 71 m shows an increase in the efficiency of RBF, reaching 72.65% compared with 71.47% without using the pipe, which can also be interpreted as the effect of the clay layer. In comparison, the increase of the depth until 91 m showed a reduction in RBF efficiency, reaching 72.29% due to groundwater interference (Figure 10).

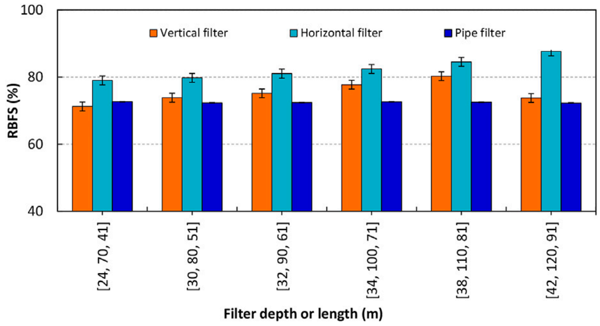

FIGURE 10
Riverbank filtration efficiency for filter depth and length.

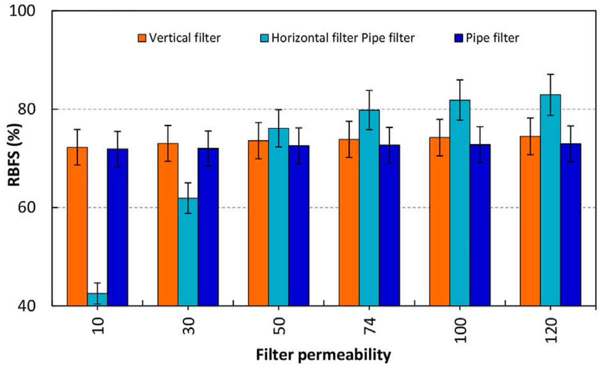

FIGURE 11
Riverbank filtration efficiency for filter permeability.

3.3 Effect of hydraulic conductivity

As previously stated, Terzaghi's law (Terzaghi, 1943) allows us to construct a gravel filter with a wide range of filter permeability values. The simulation looked at the effects of altering filter permeability [k] values by 10, 30, 50, 100, and 120 m/day versus 71.50% at this study's basic condition (74 m/day). 72.20, 73, 73.60, 74.30, and 74.50% of the RBFS was altered (Figure 11).

The RBFS for the vertical and horizontal gravel filters was 42.50, 61.90, 76.10, 81.80, and 82.90% compared to 79.80% for the base case (74 m/day). As for the drilled pipe, the RBF efficiency increased from 72.25% to 73.46%. The maximum RBFS was 74.23% at the original k with 100 m/day, but RBFS decreased again at K=120 m/day. This indicated that increasing the permeability of the filter material could increase the RBFS by the river and decrease groundwater sharing.

4 Conclusion

Using the RBF technique to overcome surface water problems could be effective. A gravel pack and pipe filter improved the technique's efficiency by certain percentages. MODFLOW software was used to investigate this efficiency by changing other parameters, including the filter width, depth, thickness, length, and permeability in vertical, horizontal gravel, and drilling pipe filters. RBF systems provide several advantages over traditional surface water treatment technologies, including a low cost and reasonably good water quality. However, because the RBF system is more unreliable than conventional systems due to its reliance on the natural environment, integrating a filter with a proposed methodology boosts the method's potential and overcomes its challenges.

In this study, increasing the vertical filter width along the riverside improves water quality, but the filter should be shallow. Increasing the thickness and length of the horizontal gravel filter uphill toward the river improves RBFS. Although the permeability of the two gravel filters was the same, the horizontal gravel filter's efficiency improved more than that of the vertical gravel filter's, especially when positioned in the well-screen layer. In addition, increasing the numbers improves the water quality, but the pipes should be somewhat shallow; yet, increasing the pipe permeability improved the RBFS. Thus, using river pipes with this technique increases the potential of this method and helps overcome the obstacles that may face the RBF system.

Data availability statement

The raw data supporting the conclusions of this article will be made available by the authors, without undue reservation.

Author contributions

Conceptualization, IA; data curation, OS and HG; formal analysis, IA; investigation, OS and HG; methodology, OS and IA; project administration, IA and MZ; resources, MZ and AK; software, OS and HG; supervision, MZ; validation, IA, OS, and HG; visualization, OS, HG, and AK; writing—original draft, IA and AK; writing—review—editing, IA, OS, HG, MZ, and AK. All authors have read and agreed to the published version of the manuscript.

Acknowledgments

The authors express their sincere appreciation to the Department of Water and Water Structures Engineering, Faculty of Engineering, Zagazig University, for using their instrument and for providing free downloads of previous research through their computer labs. AK acknowledges the Portuguese Foundation for Science and Technology (FCT) support through PTDC/CTA-OHR/30561/2017 (WinTherface).

Conflict of interest

The authors declare that the research was conducted in the absence of any commercial or financial relationships that could be construed as a potential conflict of interest.

Publisher's note

All claims expressed in this article are solely those of the authors and do not necessarily represent those of their affiliated organizations, or those of the publisher, the editors, and the reviewers. Any product that may be evaluated in this article, or claim that may be made by its manufacturer, is not guaranteed or endorsed by the publisher.

References

Abd-Elaty, I., Kushwaha, N. L., Grismer, M. E., Elbeltagi, A., and Kuriqi, A. (2022b). Cost-effective management measures for coastal aquifers affected by saltwater intrusion and climate change. *Sci. Total Environ.* 836, 155656. doi:10.1016/j.scitotenv.2022.155656

Abd-Elaty, I., and Zelenakova, M. (2022c). Saltwater intrusion management in shallow and deep coastal aquifers for high aridity regions. *J. Hydrology Regional Stud.* 40, 101026. doi:10.1016/j.ejrh.2022.101026

Abd-Elaty, I., Straface, S., and Kuriqi, A. (2021g). Sustainable saltwater intrusion management in coastal aquifers under climatic changes for humid and hyper-arid regions. *Ecol. Eng.* 171 (171), 106382. doi:10.1016/j.ecoleng.2021.106382

Abd-Elaty, I., Abd-Elhamid, H. F., and Qahman, K. (2020). Coastal aquifer protection from saltwater intrusion using abstraction of brackish water and recharge of treated wastewater: Case study of the gaza aquifer. *J. Hydrol. Eng.* 25 (7), 05020012. doi:10.1061/(asce)he.1943-5584.0001927

Abd-Elaty, I., Ghanayem, H. M., Zeleňáková, M., Mésároš, P., and Saleh, O. K. (2021a). Numerical investigation for riverbank filtration sustainability considering climatic changes in arid and semi-arid regions; case study of RBF site at Embaba, nile Delta, Egypt. *Sustainability* 13 (4), 1897. doi:10.3390/su13041897

Abd-Elaty, I., Javadi, A. A., and Abd-Elhamid, H. (2021b). Management of saltwater intrusion in coastal aquifers using different wells systems: A case study of the nile Delta aquifer in Egypt. *Hydrogeol. J.* 29, 1767–1783. doi:10.1007/s10040-021-02344-w

Abd-Elaty, I., Pugliese, L., and Straface, S. (2022a). Inclined physical subsurface barriers for saltwater intrusion management in coastal aquifers. *Water Resour. manage.* 36, 2973–2987. doi:10.1007/s11269-022-03156-7

Abd-Elaty, I., Said, A. M., Abdelaal, G. M., Zeleňáková, M., Jandora, J., and Abd-Elhamid, H. F. (2021c). Assessing the impact of lining polluted streams on groundwater quality: A case study of the eastern nile Delta aquifer, Egypt. *Water* 13 (12), 1705. doi:10.3390/w13121705

Abd-Elaty, I., Saleh, O. K., Ghanayem, H. M., Grischek, T., and Zelenakova, M. (2021d). Assessment of hydrological, geohydraulic and operational conditions at a riverbank filtration site at Embaba, Cairo using flow and transport modeling. *J. Hydrology Regional Stud.* 37, 100900. doi:10.1016/j.ejrh.2021.100900

Abd-Elaty, I., Shahawy, A. E., Santoro, S., Curcio, E., and Straface, S. (2021e). Effects of groundwater abstraction and desalination brine deep injection on a coastal aquifer. *Sci. Total Environ.* 795, 148928. doi:10.1016/j.scitotenv.2021.148928

Abd-Elaty, I., and Straface, S. (2022). “Mathematical models ensuring freshwater of coastal zones in arid and semiarid regions,” in *Earth systems protection and sustainability*. Editors J. N. Furze, S. Eslamian, S. M. Raafat, and K. Swing (Berlin, Germany: Springer). doi:10.1007/978-3-030-98584-4_3

Abd-Elaty, I., Zeleňáková, M., Krajníková, K., and Abd-Elhamid, H. F. (2021f). Analytical solution of saltwater intrusion in costal aquifers considering climate changes and different boundary conditions. *Water* 13 (7), 995. doi:10.3390/w13070995

Abd-Elaty, I., Zelenakova, M., Straface, S., Vranayová, Z., and Abu-hashim, M. (2019). Integrated modelling for groundwater contamination from polluted streams using new protection process techniques. *Water* 11 (11), 2321. doi:10.3390/w11112321

Abdalla, F., and Shamrukh, M. (2010). Riverbank filtration: Developing countries choice for water supply treatment, Egypt case.” in Proceedings of the 1 st IWAYWP. Kuala Lumpur, Malaysia, March 15–March 17

Abdel-Lah, M. A. K., and Shamrukh, M. (2006). "Riverbank filtration: A promise technique for water supply from nile, Egypt” in. Proceedings of the 7th International Symposium on Water Supply Technology). Yokohama, Japan, March 15–March 17.

Abdel-Shafy, H. I., and Aly, R. O. (2002). Water issue in Egypt: Resources, pollution and protection endeavors. *Central Eur. J. Occup. Environ. Med.* 8 (1), 3–21.

Alhejji, A., Kuriqi, A., Jurasz, J., and Abo-Elyousr, F. K. (2021). Energy harvesting and water saving in arid regions via solar PV accommodation in irrigation canals. *Energies* 14 (9), 2620. doi:10.3390/en14092620

Andrés, L., Joseph, G., and Rana, S. (2021). “The economic and health impacts of inadequate sanitation,” in *Oxford research encyclopedia of environmental science*London, UK.

Astmd5447-17 (2017). Standard guide for application of a numerical groundwater flow model to a site-specific problem, in: Proceedings of the ASTM International (West Conshohocken, PA, USA).

Carrier, W. D., III (2003). Goodbye, hazen; hello, kozeny-carman. *J. Geotech. Geoenviron. Eng.* 129 (11), 1054–1056. doi:10.1061/(asce)1090-0241(2003)129:11(1054)

Chaturvedi, M., Mishra, A., Sharma, K., Sharma, G., Saxena, G., and Singh, A. K. (2021). “Emerging contaminants in wastewater: Sources of contamination, toxicity, and removal approaches,” in *Emerging treatment technologies for waste management*. Editors I. Haq and A. S. Kalamdhad (Singapore: Springer Singapore), 103.

El-Arabi, N., Fekri, A., Zaghloul, E., and Elbeih, S. (2013). Laake A.: Assessment of groundwater movement at Giza pyramids plateau using GIS techniques. *J. Am. Sci.* 9 (6), 43–53.

El-Atfy, H. (2007). *Integrated national water resources plan in Egypt*. London, UK: Ministry Water Resour. Irrigation Alexandria Governorate.

El-Fadel, M., El-Sayegh, Y., El-Fadl, K., and Khorbotly, D. (2003). The Nile River basin: A case study in surface water conflict resolution. *J. Nat. Resour. Life Sci. Educ.* 32 (1), 107–117. doi:10.2134/jnrlse.2003.0107

El-Sheekh, M. (2009). “River nile pollutants and their effect on life forms and water quality,” in *The nile: Origin, environments, limnology and human use*. Editor H. J. Dumont (Dordrecht, Netherlands: Springer Netherlands), 395.

Ghodeif, K., Paufler, S., Grischek, T., Wahaab, R., Souaya, E., Bakr, M., et al. (2018). Riverbank filtration in Cairo, Egypt—part I: Installation of a new riverbank filtration site and first monitoring results. *Environ. Earth Sci.* 77 (7), 270. doi:10.1007/s12665-018-7450-2

Hoff, H. (2009). Global water resources and their management. *Curr. Opin. Environ. Sustain.* 1 (2), 141–147. doi:10.1016/j.cosust.2009.10.001

Javandel, I., Doughty, C., and Tsang, C.-F. (1984). *Groundwater transport: Handbook of mathematical models*. California, CA, USA: Lawrence Berkeley Lab.

Kashef, A. A. I. (1983). Salt-water intrusion in the nile Delta. *Ground Water* 21 (2), 160–167. doi:10.1111/j.1745-6584.1983.tb00713.x

Mabrouk, M., Jonoski, A., Oude Essink, H. P. G., and Uhlenbrook, S. (2018). Impacts of sea level rise and groundwater extraction scenarios on fresh groundwater resources in the nile Delta governorates, Egypt. *Water* 10 (11), 1690. doi:10.3390/w10111690

Mara, D. D., Cairncross, S., and Organization, W. H. (1989). *Guidelines for the safe use of wastewater and excreta in agriculture and aquaculture: Measures for public health protection*. Geneva, Switzerland: WHO.

Morsy, W. (2009). *Environmental management to groundwater resources for Nile Delta region*. Egypt: PhD, Cairo University.

Mwri, 2017. National water resources plan for Egypt.” in *Water for the future*. Egypt: Ministry of Water Resources and Irrigation.

Paufler, S., Grischek, T., Bartak, R., Ghodeif, K., Wahaab, R., and Boernick, H. (2018). Riverbank filtration in Cairo, Egypt: Part II—detailed investigation of a new riverbank filtration site with a focus on manganese. *Environ. Earth Sci.* 77 (8), 318. doi:10.1007/s12665-018-7500-9

Poojitha, S., Hari Prasad, K., and Ojha, C. (2022). Effect of clogging on riverbank filtration: An experimental analysis using ganges riverbed sediment. *J. Hazard. Toxic. Radioact. Waste* 26 (2), 04021065. doi:10.1061/(asce)hz.2153-5515.0000684

Ray, C., Melin, G., and Linsky, R. B. (2003). *Riverbank filtration: Improving source-water quality*. Berlin, Germany: Springer Science & Business Media.

Ray, C. (2011). “Riverbank filtration concepts and applicability to desert environments,” in *Riverbank filtration for water security in desert countries* (Berlin, Germany: Springer), 1.

Ray, C. (2008). Worldwide potential of riverbank filtration. *Clean. Technol. Environ. Policy* 10 (3), 223–225. doi:10.1007/s10098-008-0164-5

RIGW (1992). *Hydrogeological map of Egypt*. Egypt: Institute for Groundwater, National Water Research Center.

RIGW (1989). Research institute for groundwater, *Hydrogeological map of Egypt*, Egypt Cairo, scale 1:100,000,1st edn. El-Qanatir.

Said, R. (2012). *The geological evolution of the River Nile*. Berlin, Germany: Springer Science & Business Media.

Salehi, M. (2022). Global water shortage and potable water safety; Today’s concern and tomorrow’s crisis. *Environ. Int.* 158, 106936. doi:10.1016/j.envint.2021.106936

Sharma, N., Mohapatra, S., Padhye, L. P., and Mukherji, S. (2021). Role of precursors in the formation of trihalomethanes during chlorination of drinking water and wastewater effluents from a metropolitan region in Western India. *J. Water Process Eng.* 40, 101928. doi:10.1016/j.jwpe.2021.101928

Smith, H. F. (1954). *Gravel packing water wells*. London, UK: Circular.

Tang, L., Zhang, S., Zhang, X., Ma, L., and Pu, B. (2021). A review of axial vibration tool development and application for friction-reduction in extended reach wells. *J. Petroleum Sci. Eng.* 199, 108348. doi:10.1016/j.petrol.2021.108348

Terzaghi, K. (1943). *Theoretical soil mechanics*. New York, NY, USA: John Wiley & Sons, 11.

Wahaab, R. A., and Badawy, M. I. (2004). Water quality assessment of the river nile system: An overview. *Biomed. Environ. Sci.* 17 (1), 87.

Walton, W. C. (1962). *Selected analytical methods for well and aquifer evaluation*. London, UK: Bull. Ill. State Water Surv.